

Compact Coaxial Probe-Fed CP Substrate Integrated Waveguide Cavity-Backed Antenna Utilizing Slot Split Ring

Jian-Quan Huang¹, Feng Qiu¹, Chunzhi Jiang¹, Dajun Lei^{1, *},
Zhenghua Tang¹, Min Yao¹, and Qing-Xin Chu²

Abstract—A circularly polarized (CP) substrate integrated waveguide (SIW) cavity-backed slot antenna is proposed. A slot split ring (SSR) etched on the top metal surface of an SIW resonator is employed to generate the right-handed circularly polarized (RHCP) wave. The proposed antenna is excited directly by a coaxial probe with a proper distance from the symmetric axis of the SSR resonator. A prototype of the proposed CP antenna at the center frequency of 10 GHz is manufactured. As a result, the proposed antenna exhibits the advantages of both conventional planar antennas and metallic cavity backed antennas, including simple structure, compact size of $15.8 \times 15.8 \text{ mm}^2$, light weight, easy fabrication, high gain and wide axial ratio bandwidth. It is proved by experiment that an impedance bandwidth of 10.2% for the reflection coefficient less than -10 dB , an axial ratio (AR) bandwidth of 1.72% for AR less than 3 dB, and a RHCP gain 5.5 dBi have been obtained.

1. INTRODUCTION

Planar circularly polarized (CP) antennas are highly demanded in modern space and communication systems because they can not only reduce the size, volume and cost of the communication systems, but also alleviate multipath distortion and polarization mismatch losses between the receiving and transmitting antennas. Recently, numerous compact and low-profile microstrip CP antennas have been proposed. Perturbation technique, such as loading with extra stub [1], truncating corners [2], etching slots on the patch [3], and series feed coupling [4], is generally used. Meanwhile, to broaden the axial ratio bandwidth, multiple substrate layers have been applied [5–7]. However, the profiles of those antennas are high, and the antenna structures are complicated.

Conventional cavity backed antennas have many advantages such as low mutual coupling between antenna elements, low back lobes and gain enhancement. However, traditional cavities employed in antenna are relatively bulky and difficult to integrate with circuits. Substrate integrated waveguide (SIW) antennas have the advantage of low cost, easy integration to circuits and easy fabrication with printed circuit board (PCB) process. Several SIW cavity-backed antenna configurations have been reported. In [8] and [9], a SIW cavity-backed ring slot antenna unified with an SIW feeding network was proposed [8, 9]. By introducing a simply shorting via, the CP generation and a broadband impedance matching characteristic were accomplished. In [10], by exciting two orthogonal resonant modes of an SIW resonator with four radiating slots, a CP SIW slot antenna with high gain was designed. Crossed slot structures were also adopted to achieve the CP radiation characteristic [11–13]. In [12], the gain of a CP x-slot antenna was enhanced by adding a surface mounted horn. Some authors designed new feeding structures to widen the AR bandwidth. In [14], the authors designed a novel feeding transition from stripline to SIW to meliorate the operating bandwidth, and a broad AR bandwidth of the proposed

Received 11 April 2016, Accepted 18 May 2016, Scheduled 28 May 2016

* Corresponding author: Dajun Lei (Leidajun@126.com).

¹ School of Electronic Information and Electrical Engineering, Xiangnan University, Chenzhou, Hunan, China. ² School of Electronic and Information Engineering, South China University of Technology, Guangzhou, China.

CP antenna was obtained. However, those SIW cavity-backed antennas were usually loaded with extra feeding networks, which make the antennas larger and not suitable for array application.

In this paper, a circularly polarized substrate integrated waveguide cavity-backed antenna based on a slot split ring (SSR) is proposed. A coaxial probe with a proper offset from the symmetric axis of the SSR is employed to feed the circular SIW cavity-backed antenna directly. Two orthogonal modes of the SSR and SIW resonators are excited, so that circular polarization can be achieved. The total size of antenna is only $15.8 \times 15.8 \text{ mm}^2$ owing to no extra SIW feed structure.

2. ANTENNA CONFIGURATION AND DESIGN

A configuration of the proposed antenna is illustrated in Figure 1. A circular cavity with radius of r_{SIW} is created by an annular array of vertical metallic vias with the diameter of d_2 and distance of p_v penetrating through a substrate FR-4 PCB with the relative permittivity 4.4, loss tangent 0.02, and height $h = 1.57 \text{ mm}$. A slot split ring resonator (SSRR) with radius of r_{SSR} and split of w_1 is etched on the upper metal layer of the SIW cavity and excited by a coaxial probe at the distance of x_{offset} away from the center of the SIW.

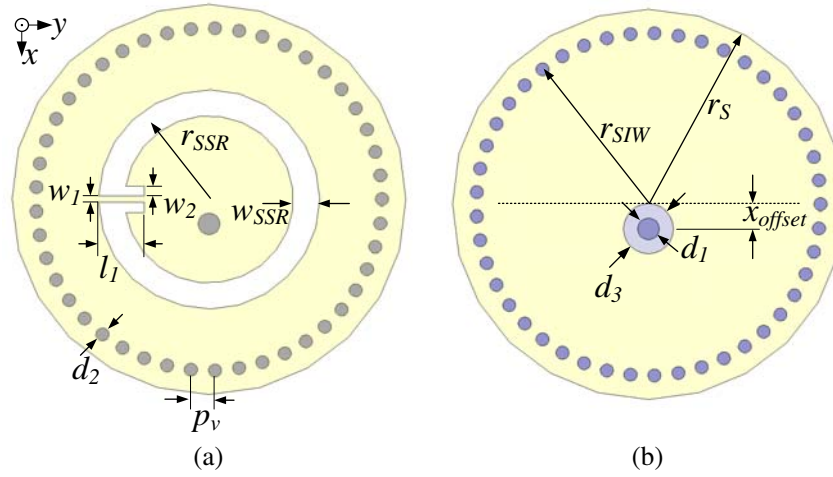


Figure 1. (a) Top view and (b) bottom view of the proposed antenna ($r_S = 9.00 \text{ mm}$, $r_{SIW} = 7.90 \text{ mm}$, $r_{SSR} = 4.45 \text{ mm}$, $w_{SSR} = 1.20 \text{ mm}$, $w_1 = 0.30 \text{ mm}$, $w_2 = 0.45 \text{ mm}$, $l_1 = 1.60 \text{ mm}$, $d_1 = 1.00 \text{ mm}$, $d_2 = 2.30 \text{ mm}$, $d_3 = 0.60 \text{ mm}$, $p_v = 1.10 \text{ mm}$, $x_{offset} = 1.12 \text{ mm}$).

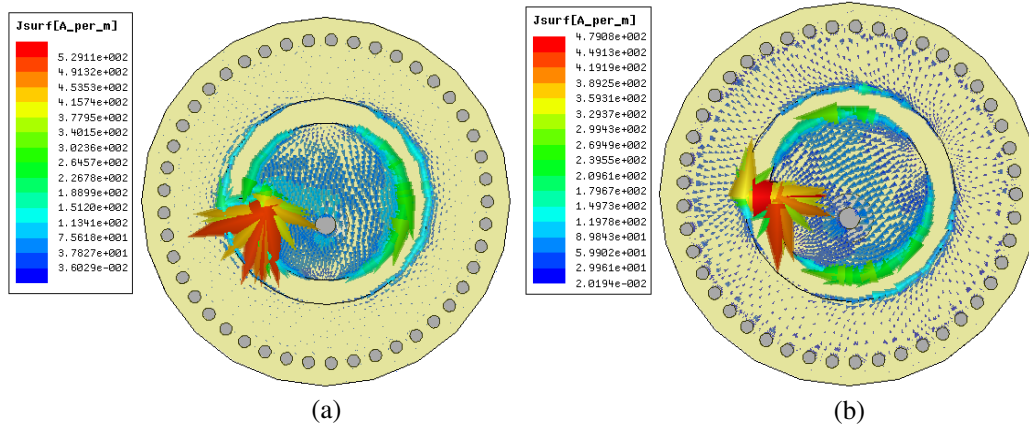


Figure 2. Current distributions on the top metal layer of SIW cavity at each resonant frequency (a) the first resonant mode at 9.68 GHz of the slot split ring resonator and (b) the second resonant TM_{010} -mode at 10.20 GHz of the SIW resonator.

Figure 2 depicts the simulated electric currents of the antenna at two resonant frequencies. As shown in Figure 2(a), the lower frequency f_L is ascribed to the resonance of the SSRR (denoted as SSRR mode). It can be seen that the terminals and center of the SSRR have the strongest electric current at this resonance frequency. f_L can be estimated by the following equation [15]:

$$f_L = \frac{c}{2\pi \cdot r_{\text{SSRR}} - w_1 + 2(l_1 - w_{\text{SSRR}})} \times \frac{1.2}{\sqrt{\epsilon_{\text{eff}}}} \quad (1)$$

where c is the speed of light in free space, and $\epsilon_{\text{eff}} = 2\epsilon_r/(1 + \epsilon_r)$ is the effective relative permittivity considering the presence of different dielectric media between the slot and the ground. The simulated electric current distribution of the top layer of SIW resonator at higher resonant frequency f_H is plotted in Figure 2(b). It is due to the resonance of SIW resonator (denoted as SIW mode) at its fundamental mode (TM₀₁₀-like mode). Considering the perturbation by the split slot ring, the resonant frequency f_H is given by [16]

$$f_H = \frac{0.345c}{r_{\text{SIW}}\sqrt{\epsilon_{\text{eff}}}} \quad (2)$$

where c and ϵ_{eff} are the same as Equation (1). It is noted that the total E -fields on the split ring slot on the top layer is roughly orthogonal to those at lower resonance frequency f_L . To obtain a CP radiation, the offset x_{offset} of coaxial probe away from the symmetric axis of SSRR is chosen carefully to excite two electromagnetic orthogonal components with equal magnitudes and phase difference of 90°. The proposed antenna radiates a right-hand circularly polarized (RHCP) wave. The left-hand circularly polarized (LHCP) wave can be obtained by mirroring the coaxial probe with respect to y -axis.

The circular polarization band is between the lower resonant frequency and the higher one. Thus, the operating frequency of the proposed antenna is mainly influenced by radius r_{SIW} of the SIW resonator and radius r_{SSRR} of the split slot ring. Figure 3 shows the influence of the cavity and slot

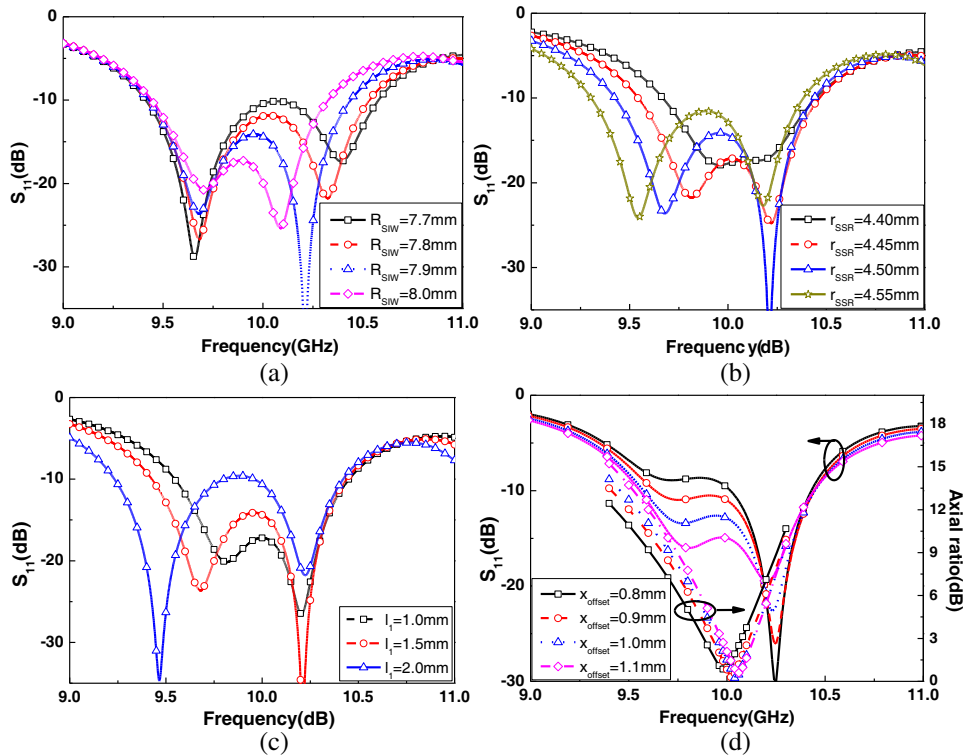


Figure 3. Effects of selected antenna parameters on reflection coefficient and axial ratio: (a) diameter r_{SIW} of SRR; (b) width w_{SSRR} of SIW cavity; (c) length l_1 of stub and (d) distance x_{offset} of coaxial probe away from the center of SIW cavity.

dimensions on the two resonant frequencies. Variation of S_{11} versus frequency for different values of cavity radius r_{SIW} is depicted in Figure 3(a). It can be seen by increasing r_{SIW} , and higher resonant frequency is decreased, and lower resonant frequency is also affected a bit. Moreover, the radius, r_{SRR} , has a great effect on S_{11} of the slot antenna. Variation of S_{11} versus frequency for different values of r_{SRR} is illustrated in Figure 3(b). It can be observed that the effect of a small change of r_{SRR} on the lower resonant frequency is more significant than those on the higher one. Variation of l_1 also slightly affects lower resonant frequency and matching as shown in Figure 3(c). The distance of the coaxial probe x_{offset} has much influence on magnitudes of two resonant modes and input impedance of the antenna. Consequently, by tuning these parameters the axial ratio and impedance bandwidth of the antenna can be adjusted, as shown in Figure 3(d). According to the above discussion, in order to achieve a wide axial bandwidth and low return loss, appropriate dimensions of the cavity, split slot ring and location of the excited probe can be achieved by using Ansoft HFSS. All optimized parameters of the proposed antenna are listed in Figure 1.

3. EXPERIMENTAL RESULTS AND DISCUSSION

To demonstrate performances of the proposed antenna, a prototype has been successfully fabricated, as shown in Figure 4. The S-parameter was measured by Agilent vector network analyzer PNA N5230C. Both measured and simulated results obtained by Ansoft HFSS are depicted in Figure 5. The measured result agrees well with the simulated one. The measured impedance bandwidth of 10.12% (for $S_{11} < -10$ dB) is greater than the simulated one of 10.1%. The slight difference is mainly caused by fabrication tolerances, and probably a slightly difference of the relative permittivity of the practical substrate compared to the simulated one. The AR, gain and radiation patterns of the proposed antenna were measured in an anechoic chamber by Agilent vector network analyzer ENA E5071. Simulated and measured results of the AR at the boresight direction (z -axis direction) versus frequency are shown in Figure 5. Again measured results are in agreement with the simulated ones. The measured AR bandwidth is 1.72% (for AR < 3 dB), which is much less than the fractional impedance bandwidth. The simulated and the measured gains at the boresight direction are also shown in Figure 5. It is seen that the proposed antenna has 5.5 dBi maximum gain within 9.3 to 10.5 GHz at the boresight direction, a very stable 3 dB gain bandwidth of 1.02 GHz. The measured realized gain of the antenna at frequency 10 GHz at the boresight direction is 5.0 dBi, which is slightly lower than that of the simulated result. The simulated and measured far-field radiation patterns in two orthogonal cutting planes at the frequency 10 GHz are illustrated in Figure 6. It is proved that the antenna radiates a RHCP wave with low cross-polarization at the boresight direction. The maximum of radiation in E -plane xoz is slightly shifted about 12.5° .



Figure 4. Photo of the fabricated CP antenna.

Table 1 compares the proposed antenna with the previous designs. It can be seen that the proposed antenna has the advantages of compact size, wide impedance matching bandwidth and AR bandwidth, easy integration with planar circuits due to the flexible feed structure. Moreover, compared to [11], the proposed antenna has a wider operation bandwidth and 80.8% smaller planar size.

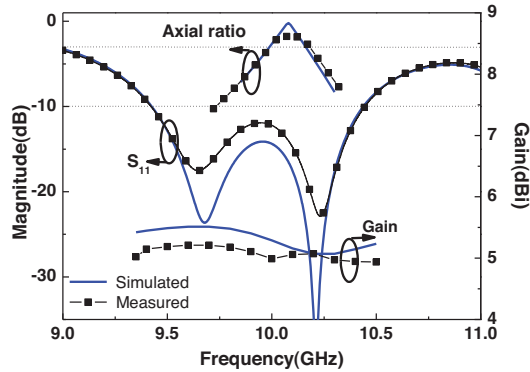


Figure 5. Measured and simulated reflect coefficient, axial ratio and gain of the proposed antenna.

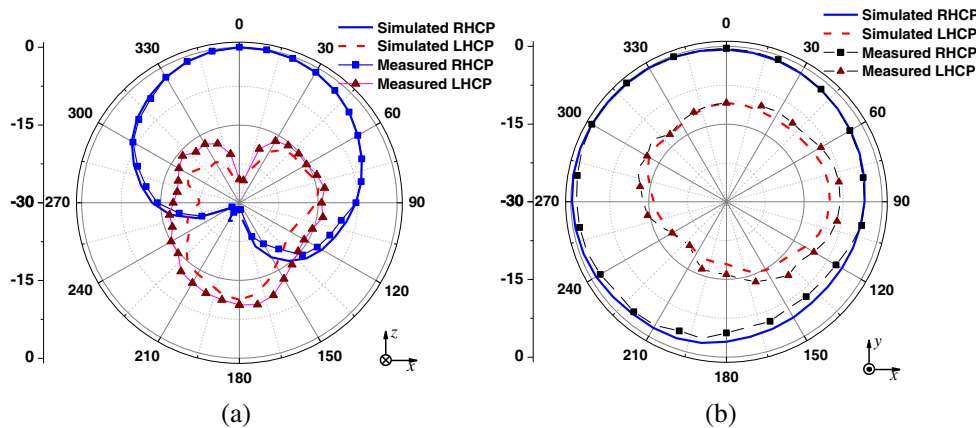


Figure 6. Measured and simulated radiation of the proposed antenna at 10 GHz. (a) xoz plane and (b) xoy plane.

Table 1. Comparison of the proposed CP SIW antenna with previously published ones.

ref	size	BW %	AR bandwidth%	Peak Gain (dBi)	Feed type
[8]	$0.88\lambda_0 \times 0.54\lambda_0$	9	2.6	8.2	Coax-to-SIW
[9]	$1.27\lambda_0 \times 0.83\lambda_0$	12.86	2.3	5.75	Microstrip-to-SIW
[11]	$1.21\lambda_0 \times 1.21\lambda_0$	2.85	0.6	7.8	Microstrip-to-SIW
[13]	$0.53\lambda_0 \times 0.53\lambda_0$	1.8	0.8	6.5	Microstrip direct
This work	$0.53\lambda_0 \times 0.53\lambda_0$	10.2	1.72	5.5	Coax direct

4. CONCLUSIONS

In this paper, a very compact X-band circular polarized split-ring-slot SIW back-cavity antenna has been proposed. Two orthogonal modes have been excited by a coax with proper offset from the symmetric axis of SSR. Consequently, the circular polarization wave is generated. The antenna exhibits the further advantage of small size and light weight. Experimental results prove that the antenna achieves the impedance bandwidth of 10.12% (for $S_{11} < -10$ dB), AR bandwidth of 1.72% (for $AR < 3$ dB), realized RHCP gain 5.0 dBi, and low level of cross-polarization at the boresight direction. The proposed configuration can be applied to array antennas for satellite communication.

ACKNOWLEDGMENT

This work was supported by Science and Technology Innovative Research Team in Higher Educational Institutions and the Research Foundation of Education Department (Grant No. 14C1061) of Hunan Province.

REFERENCES

1. Wong, K. L. and Y. F. Lin, "Circularly polarized microstrip antenna with a tuning stub," *Electron. Lett.*, Vol. 34, No. 9, 831–832, Apr. 1998.
2. Chen, W. S., C. K. Wu, and K. L. Wong, "Single-feed square-ring microstrip antenna with truncated corners for compact circular polarization operation," *Electron. Lett.*, Vol. 34, No. 11, 1045–1047, May 1998.
3. Lam, K. Y., K. M. Luk, K. F. Lee, H. Wong, and K. B. Ng, "Small circularly polarized U-slot wideband patch antenna," *IEEE Antennas Wireless Propag. Lett.*, Vol. 10, 87–90, 2011.
4. Row, J. S., "The design of a squarer-ring slot antenna for circular polarization," *IEEE Trans. Antennas Propag.*, Vol. 53, No. 6, 1967–1972, Jun. 2005.
5. Buffi, A., R. Caso, M. R. Pino, P. Nepa, and G. Manara, "Single-feed circularly polarized aperture-coupled square ring slot microstrip antenna," *Electron. Lett.*, Vol. 46, No. 4, 268–269, Feb. 2010.
6. Chung, K. L., "A wideband circularly polarized H-shaped patch antenna," *IEEE Trans. Antennas Propag.*, Vol. 58, No. 10, 3379–3383, Oct. 2010.
7. Rao, P. H., V. F. Fusco, and R. Cahill, "Wide-band linear and circularly polarized patch antenna using a printed stepped T-feed," *IEEE Trans. Antennas Propag.*, Vol. 50, No. 3, 356–361, Mar. 2002.
8. Lacik, J., "Circularly polarised SIW square ring-slot antenna for X-band applications," *Microwave Opt Technol Lett.*, Vol. 54, No. 11, 2590–2594, Nov. 2012
9. Kim, D., J. W. Lee, C. S. Cho, and T. K. Lee, "X-band circular ring slot antenna embedded in single-layered SIW for circular polarisation," *Electron Lett.*, Vol. 45, No. 13, 668–669, June 2009.
10. Hao, Z. C., X. Liu, X. Huo, et al., "Planar high-gain circularly polarized element antenna for array applications," *IEEE Transactions on Antennas & Propagation*, Vol. 63, No. 5, 1937–1948, May 2015.
11. Elboushi, A., O. Haraz, and A. Sebak, "High gain circularly polarized slot-coupled antenna for millimeter wave applications," *Microwave Opt Technol Lett.*, Vol. 56, No. 11, 2522–2526, Aug. 2014.
12. Pablo, S. O. and L. M. C. José, "Novel four cross slot radiator with tuning vias for circularly polarized SIW linear array," *IEEE Trans. Antennas Propag.*, Vol. 62, No. 4, 2271–2275, Apr. 2014.
13. Luo, G. Q., Z. F. Hu, Y. Liang, L. Y. Yu, and L. L. Sun, "Development of low profile cavity backed crossed slot antennas for planar integration," *IEEE Trans. Antennas Propag.*, Vol. 57, No. 10, 2972–2979, Oct. 2009.
14. Gao, F., F. Zhang, L. Lu, and Y. C. Jiao, "Wideband Circularly polarised SIW antenna," *Microwave Opt. Technol. Lett.*, Vol. 56, No. 11, 2539–2542, Aug. 2014.
15. Chen, W. S., C. C. Huang, and K. L. Wong, "Microstrip-line-fed printed shorted ring-slot antennas for circular polarization," *Microwave Opt. Technol. Lett.*, Vol. 31, No. 2, 137–140, Aug. 2001.
16. Rao, J. S. and B. N. Das, "Impedance characteristics of transverse slots in the ground plane of a stripline," *Proc. IEE*, Vol. 125, No. 1, 29–32, Jan. 1978.